Zero-phonon line and fine structure of the yellow luminescence band in GaN

M. A. Reshchikov,[1,*] J. D. McNamara,[1] F. Zhang,[2] M. Monavarian,[2] A. Usikov,[3,4] H. Helava,[3] Yu. Makarov,[3] and H. Morkoç[2]

[1]*Department of Physics, Virginia Commonwealth University, Richmond, Virginia 23284, USA*

[2]*Department of Electrical and Computing Engineering, Virginia Commonwealth University, Richmond, Virginia 23284, USA*

[3]*Nitride Crystals, Inc., 181E Industry Court, Suite. B, Deer Park, New York 11729, USA*

[4]*Saint-Petersburg National Research University of Information Technologies, Mechanics and Optics, 49 Kronverkskiy Avenue, 197101 Saint Petersburg, Russia*

(Received 6 April 2016; revised manuscript received 17 June 2016; published 5 July 2016)

The yellow luminescence band was studied in undoped and Si-doped GaN samples by steady-state and time-resolved photoluminescence. At low temperature (18 K), the zero-phonon line (ZPL) for the yellow band is observed at 2.57 eV and attributed to electron transitions from a shallow donor to a deep-level defect. At higher temperatures, the ZPL at 2.59 eV emerges, which is attributed to electron transitions from the conduction band to the same defect. In addition to the ZPL, a set of phonon replicas is observed, which is caused by the emission of phonons with energies of 39.5 meV and 91.5 meV. The defect is called the YL1 center. The possible identity of the YL1 center is discussed. The results indicate that the same defect is responsible for the strong YL1 band in undoped and Si-doped GaN samples.

DOI: 10.1103/PhysRevB.94.035201

I. INTRODUCTION

Understanding and identifying point defects in GaN is important for improving the material quality as well as for increasing the efficiency of III-nitride-based light-emitting devices and the breakdown voltage of GaN-based high-power devices. First-principles calculations of point defects in semiconductors employ various approximations and corrections, and specific approaches on how to use these corrections are frequently debated [1]. In this situation, reliable experimental data are needed to find the best theoretical approach. In spite of many years of research, a majority of the point defects in undoped GaN are still not understood, including the notorious yellow luminescence (YL) band commonly observed in photoluminescence (PL) spectra for a variety of GaN samples grown by different techniques [2]. In the past, several impurities, native defects, and defect complexes were proposed by researchers as the defects responsible for the YL band. Currently, either isolated carbon in a nitrogen site (C_N) [3], a carbon-oxygen complex (C_NO_N) [4,5], or other complexes such as V_{Ga}-3H or $V_{Ga}O_N$-2H [6], are considered as the main candidates for the defects which produce the YL band. Since several types of defects may cause broad bands with similar position and shape, precise experimental measurements are required to distinguish the defects.

Modern first-principles calculations predict the thermodynamic transition levels and the optical transition energies for point defects. The latter can be compared to the position of a PL band maximum, while the former should be compared to the position of the zero-phonon line (ZPL). To the best of our knowledge, the ZPL for the YL band has not been directly observed, and its position was predicted to occur at 2.64–2.70 eV [7,8]. This value was estimated as the photon energy roughly between the high-energy "edge" of the broad YL band and the low-energy "edge" of the characteristic PL excitation band, although the PL and PL excitation bands did not show abrupt edges. In this work, we report on the observation of the ZPL at 2.590 ± 0.003 eV and the fine structure of the YL band caused by a superposition of PL lines related to emission of pseudolocal and lattice phonons.

II. EXPERIMENT

The fine structure of the YL band was detected in more than ten GaN samples grown on *c*-plane sapphire. Of these, three representative GaN samples were analyzed in more detail in this work (Table I). A 24-μm-thick, unintentionally doped GaN layer (sample H2057) with a room-temperature concentration of free electrons $n = 6 \times 10^{16}$ cm^{-3} was grown by hydride vapor phase epitaxy (HVPE) at Nitride Crystals, Inc. A Si-doped GaN layer (sample cvd3784) with GaN layer thickness of 12.5 μm was grown by metalorganic chemical vapor deposition (MOCVD) at VCU. A 1.9-μm-thick, unintentionally doped GaN layer (sample EM1256) was grown by MOCVD at EMCORE Corporation. The dominant acceptor impurity in the last sample is carbon with a concentration of 4×10^{16} cm^{-3}, and other details for this sample can be found in Refs. [4] and [5]. The concentrations of Si, C, and O in Table I are estimated from dedicated secondary ion mass-spectrometry (SIMS) measurements conducted by Evans Analytical Group. The concentration of carbon in sample H2057 is apparently lower than 5×10^{15} cm^{-3}, which is the detection limit in these measurements.

Steady-state PL (SSPL) was excited with a He-Cd laser (30 mW, 325 nm), dispersed by a 1200 rules/mm grating in a 0.3 m monochromator and detected by a cooled photomultiplier tube. Time-resolved PL (TRPL) was excited with a pulsed nitrogen laser (pulses with a wavelength of 337 nm, a duration of 1 ns, and repetition frequency of 6 Hz) and analyzed with an oscilloscope. The PL spectra were corrected for the response of the optical system. By using the 325.03 nm and 633.82 nm lines from He-Cd and He-Ne lasers, the photon energies are verified to have an accuracy of better than 0.5 meV. The absolute internal quantum efficiency of PL, η, is defined as $\eta = I^{PL}/G$, where I^{PL} is the integrated PL intensity from a

*mreshchi@vcu.edu

TABLE I. Parameters of select GaN samples and their PL features at $T = 18$ K.

Sample	Growth	n from	[Si] from	[O] from	[C] from		DBE	UVL	
number	method	Hall (cm^{-3})	SIMS (cm^{-3})	SIMS (cm^{-3})	SIMS (cm^{-3})	DBE (eV)	FWHM (meV)	DAP (eV)	e-A (eV)
H2057	HVPE	6×10^{16}	5×10^{16}	2×10^{16}	$<5 \times 10^{15}$	3.473	3.4	3.263	
cvd3784	MOCVD	3×10^{18}	4×10^{18}	1×10^{16}	4×10^{16}	3.479	12		3.288
EM1256	MOCVD	2×10^{16}	3×10^{16}	5×10^{16}	4×10^{16}	3.4795	6	3.268	

particular PL band and G is the concentration of electron-hole pairs created by the laser per second in the same volume. To find η for a particular PL band, we compared its integrated intensity with the PL intensity obtained from a calibrated GaN sample [9,10].

III. RESULTS

Figure 1 shows the PL spectra from three GaN samples measured in identical conditions at low temperature (T) and low excitation power density (P_{exc}). For undoped GaN grown by HVPE (H2057), the strongest PL line, identified as the donor-bound exciton (DBE), is observed at 3.473 eV with a full width at half maximum (FWHM) of 3.4 meV (the inset in Fig. 1). The ultraviolet luminescence (UVL) band with a maximum at 3.263 eV is followed by three LO phonon replicas at distance multiples of 91.5 meV. At lower photon energies, the YL and red luminescence (RL) bands overlap. The parameters of the DBE and UVL lines for MOCVD GaN samples are given in Table I.

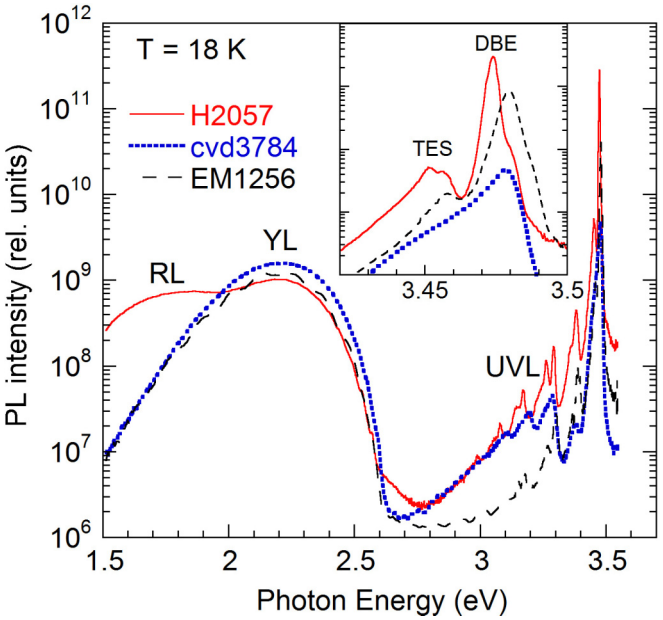

FIG. 1. PL spectrum for undoped GaN grown by HVPE (sample H2057), Si-doped GaN grown by MOCVD (sample cvd3784), and MOCVD-grown undoped GaN (sample EM1256). $T = 18$ K, $P_{exc} = 0.001$ W/cm^2. The inset shows details in the region of the exciton emission obtained at $P_{exc} = 0.2$ W/cm^2, including the donor-bound-exciton (DBE) and two-electron-satellite (TES) lines for undoped GaN and a broad exciton line for Si-doped GaN. $\eta = 20\%$ (exciton), 0.07% (UVL), 3% (YL), and 2% (RL) for sample H2057; $\eta = 1\%$ (exciton), 0.05% (UVL), and 5% (YL) for sample cvd3784; and $\eta = 7\%$ (exciton), 0.01% (UVL), and 4% (YL) for sample EM1256.

In order to resolve the YL and RL bands, their shapes, $I^{PL}(\hbar\omega)$, were simulated with the following formula derived from a one-dimensional configuration coordinate model [11]:

$$I^{PL}(\hbar\omega) = I^{PL}_{max} \exp\left[-2S_e\left(\sqrt{\frac{E_0^* - \hbar\omega}{\Delta E}} - 1\right)^2\right]. \quad (1)$$

Here, I^{PL}_{max} is the intensity of the PL band maximum, S_e is the Huang-Rhys factor for the excited state, $\Delta E = E_0^* - \hbar\omega_{max}$ is the relaxation energy in the ground state (Stokes shift), $\hbar\omega$ and $\hbar\omega_{max}$ are the PL photon energy and position of the band maximum, and $E_0^* = E_0 + 0.5\hbar\Omega$, where E_0 is the ZPL energy and $\hbar\Omega$ is the energy of the effective phonon mode in the excited state [12]. Note that the shape of a broad PL band is uniquely described by just two parameters: S_e and ΔE. Below, we will analyze in more detail the shape of the YL band and the fine structure on its high-energy side for three types of GaN samples.

A. Undoped GaN grown by HVPE

Figure 2 shows the low-temperature PL spectra (SSPL and TRPL) from an undoped GaN layer grown by HVPE. The YL band with a maximum at 2.20 eV overlaps with the RL band at its low-energy side and with a green luminescence (GL) band at its high-energy side. The GL band is very weak at low excitation intensities. However, its contribution increases with increasing excitation intensity, and it can also be observed as an isolated band in TRPL spectra for time delays shorter than 10 μs. The YL intensity abruptly drops at photon energies close to 2.57 eV, especially in the TRPL spectrum where the contribution of the GL band is negligible. We identify the peak at 2.57 eV as the ZPL of the YL band. Another peak can be seen at 2.53 eV and is identified as the first phonon replica (labeled 10). Similar PL spectra were observed in eight other HVPE GaN samples, where the ZPL of the YL band (albeit less well resolved) could be detected.

B. Undoped GaN grown by MOCVD

The YL band in MOCVD-grown GaN samples appears as an isolated band with asymmetric shape ($S_e = 7.4$ and $\Delta E = 0.46$ eV) and a maximum at 2.20 eV (in unstrained GaN with a low concentration of shallow donors) or at slightly higher photon energies (up to ~2.22 eV in undoped GaN with large biaxial strain in a thin GaN layer on sapphire substrate or in GaN samples with a high concentration of shallow donors). For the undoped MOCVD-grown sample EM1256, the YL band can be fitted using Eq. (1) with $\hbar\omega_{max} = 2.203$ eV and $E_0^* = 2.663$ eV (Fig. 3). At the high-energy side, the ZPL is observed at about 2.58 eV with an intensity of 1% of the YL

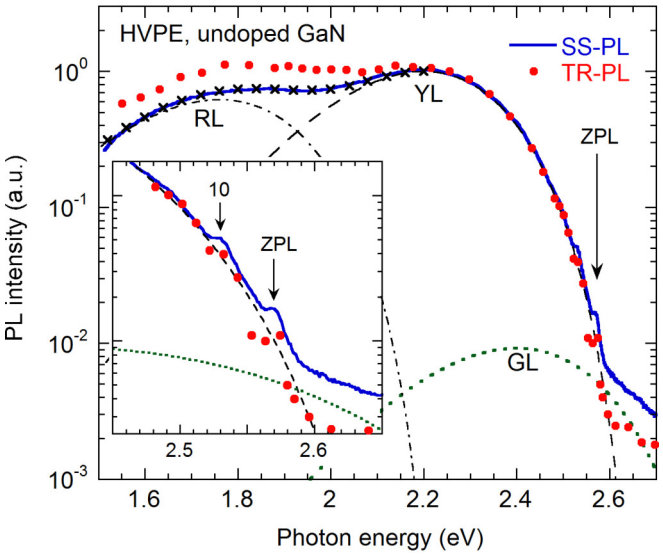

FIG. 2. Normalized PL spectrum at $T = 18\,\mathrm{K}$ and $P_{\mathrm{exc}} = 1\,\mathrm{mW/cm^2}$ from undoped GaN grown by HVPE. The solid line is the SSPL spectrum. The dotted, dashed, and dash-dotted lines are calculated for the GL, YL, and RL bands, respectively, using Eq. (1) with the following parameters: $I^{\mathrm{PL}}_{\mathrm{max}} = 0.0092$, $S_e = 8.5$, $E^*_0 = 2.93\,\mathrm{eV}$, $\hbar\omega_{\mathrm{max}} = 2.40\,\mathrm{eV}$ for the GL band, $I^{\mathrm{PL}}_{\mathrm{max}} = 1$, $S_e = 7.4$, $E^*_0 = 2.66\,\mathrm{eV}$, $\hbar\omega_{\mathrm{max}} = 2.20\,\mathrm{eV}$ for the YL band, and $I^{\mathrm{PL}}_{\mathrm{max}} = 0.62$, $S_e = 6.5$, $E^*_0 = 2.22\,\mathrm{eV}$, $\hbar\omega_{\mathrm{max}} = 1.76\,\mathrm{eV}$ for the RL band. The $\times$ symbols show the sum of the calculated YL and RL bands. The filled circles are the TRPL spectrum taken 1 ms after a laser pulse. The inset shows a zoomed-in spectrum near the ZPL.

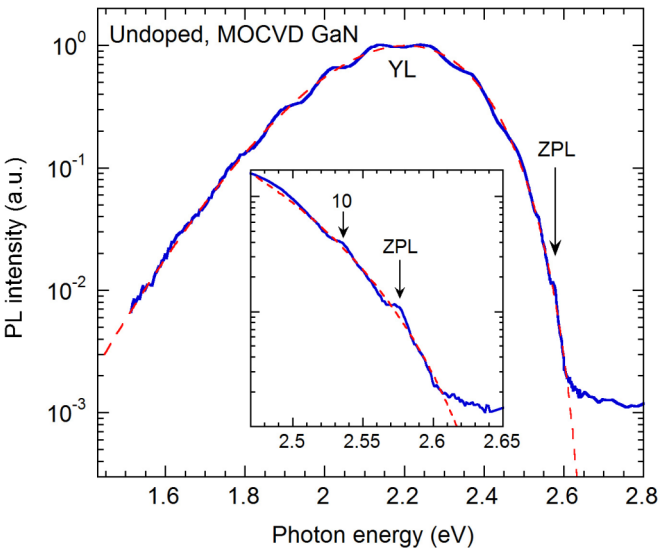

FIG. 3. Normalized SSPL spectrum at $T = 18\,\mathrm{K}$ and $P_{\mathrm{exc}} = 0.03\,\mathrm{mW/cm^2}$ from undoped GaN grown by MOCVD (sample EM1256). The long-range oscillations (with separations between maxima of 120 meV) are caused by Fabry-Pérot interference in the 1.9-μm-thick GaN layer. The dashed line is calculated using Eq. (1) with the following parameters: $I^{\mathrm{PL}}_{\mathrm{max}} = 1$, $S_e = 7.4$, $E^*_0 = 2.663\,\mathrm{eV}$, $\hbar\omega_{\mathrm{max}} = 2.203\,\mathrm{eV}$. The inset shows a zoomed-in spectrum near the ZPL.

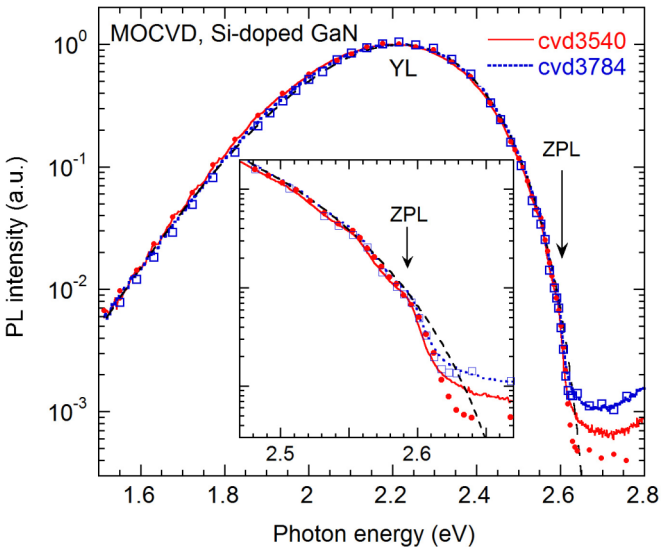

FIG. 4. Normalized PL spectra at $T = 18\,\mathrm{K}$ and $P_{\mathrm{exc}} = 1\,\mathrm{mW/cm^2}$ from two Si-doped GaN samples grown by MOCVD. The solid and dotted lines are the SSPL spectra for samples cvd3540 and cvd3784, respectively. The filled circles and empty squares are the TRPL spectra for samples cvd3540 and cvd3784, respectively, taken 5–10 μs after a laser pulse. The dashed line is calculated using Eq. (1) with the following parameters: $I^{\mathrm{PL}}_{\mathrm{max}} = 1$, $S_e = 7.4$, $E^*_0 = 2.68\,\mathrm{eV}$, $\hbar\omega_{\mathrm{max}} = 2.22\,\mathrm{eV}$. The inset shows a zoomed-in spectrum near the ZPL.

band maximum. The first phonon replica of the ZPL can be resolved at 2.54 eV (the inset to Fig. 3), which is very similar to the fine structure of the YL band in HVPE-grown GaN. The observed fine structure of the YL band serves as a fingerprint of the defect responsible for the YL band. Among other characteristics of this defect (established for sample EM1256) is the electron-capture coefficient $C_{nA} = 1 \times 10^{-13}\,\mathrm{cm^3/s}$ determined from TRPL measurements and the hole-capture coefficient $C_{pA} = 6 \times 10^{-7}\,\mathrm{cm^3/s}$ determined from the thermal quenching of the YL band at temperatures above 450 K with an activation energy of about 850 meV.

C. Si-doped GaN grown by MOCVD

The YL band in seven Si-doped GaN samples (with n from 6×10^{16} to $7 \times 10^{18}\,\mathrm{cm^{-3}}$) is very similar to that in undoped GaN, but it is slightly shifted to higher photon energies ($\Delta E = 0.46\,\mathrm{eV}$ and $\hbar\omega_{\mathrm{max}} = 2.22\,\mathrm{eV}$ for sample cvd3784). The YL band intensity abruptly drops at about 2.6 eV, and we attribute this feature to its ZPL (Fig. 4). The shape of the YL band is the same in the SSPL and TRPL spectra (at different time delays), which indicates that only one defect contributes to the spectrum between 1.5 and 2.6 eV. The shift of the YL band by 0.02 eV to higher energies in Si-doped GaN as compared to undoped GaN can be attributed to the corresponding shift of the Fermi level in degenerate, n-type GaN:Si. Thus, we conclude that the strong YL bands in Si-doped and undoped GaN samples are identical and caused by the same defect.

D. Fine structure of the YL band

To better observe the fine structure of the YL band on its high-energy side for all three types of GaN samples, we

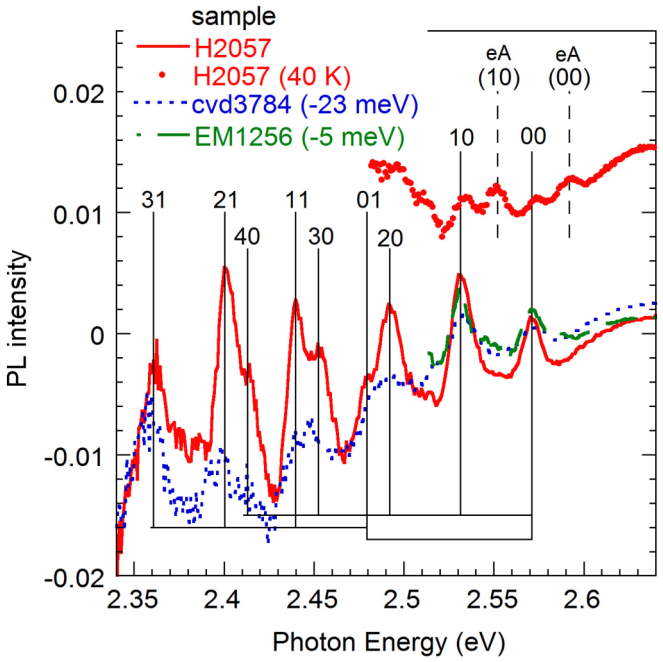

FIG. 5. SSPL spectra from three GaN samples after subtracting the smooth components which are calculated using Eq. (1). $P_{exc} = 0.5\,mW/cm^2$. The spectra for MOCVD-grown samples are shifted by 23 meV (cvd3784) and 5 meV (EM1256) to lower energy in order to match the position of the ZPL in an HVPE-grown GaN sample (H2057) at 2.571 eV. The ZPL and its phonon replicas are labeled as mn, where m indicates the number of emitted pseudolocal phonons (with energy 39.5 meV) and n indicates the number of emitted LO lattice phonons (with energy 91.5 meV). The top spectrum (filled circles, sample H2057) is obtained at $T = 40$ K and shifted vertically by 0.014 for clarity.

subtracted the smooth component obtained with Eq. (1) from the as-measured PL spectrum. The results for the three representative samples are shown in Fig. 5. For clarity, the spectra for MOCVD-grown samples are redshifted by 23 meV (cvd3784) and 5 meV (EM1256) to match the peaks in the HVPE-grown sample. We will first analyze in detail HVPE GaN samples and then briefly compare them with MOCVD GaN samples.

The fine structure of the YL band in undoped GaN (H2057) at $T = 18$ K includes the ZPL at 2.571 ± 0.001 eV followed by a superposition of two types of phonon replicas: a pseudolocal mode with phonon energy of 39.5 ± 0.5 meV and an LO lattice mode with phonon energy of 91.5 ± 0.5 meV. The experiment and the above-described analysis have been repeated many times to improve the statistical data, and the results are reproducible. The phonon replicas in Fig. 5 are labeled with indices mn, where m and n indicate the number of emitted pseudolocal and LO lattice phonons, respectively.

With increasing excitation intensity at $T = 18$ K, the ZPL and the phonon replicas shift to higher photon energies. The total shift is 5–6 meV when the excitation power density is varied by four orders of magnitude. The shift is nearly identical to the shift of the UVL band peaks. In the latter case, it is explained by the donor-acceptor-pair (DAP) nature of the UVL band at low temperatures. Emission from distant pairs (contributing at lower photon energies) saturates at lower excitation intensities as compared to close pairs (contributing at higher photon energies due to higher Coulomb interaction), and the PL band maximum gradually shifts to higher photon energies [2,13].

With increasing temperature, the amplitude of the fine structure of the YL band gradually decreases, and the lines slightly shift to higher energies (by 2–3 meV at 40 K). Simultaneously, a very similar set of lines appears, with photon energies shifted to higher energies by 17–19 meV from the low-temperature set. An example for sample H2057 is shown in Fig. 5 with filled circles for $T = 40$ K, where two sets coexist and the first line is observed at 2.593 eV. At $T > 60$ K, the fine structure disappears. The temperature behavior of the YL band is again very similar to that of the UVL band, in which the DAP peaks are replaced with peaks caused by transitions from the conduction band to the shallow acceptor (e-A transitions) with increasing temperature [2]. In particular, the DAP-related ZPL of the UVL band for sample H2057 gradually shifts from 3.262 eV to 3.2645 eV with increasing temperature from 18 to 40 K, and the (e-A)-related ZPL emerges at 3.2835 eV at 40 K. The distance between the DAP and e-A lines is 17–19 meV for both the UVL and YL bands, for temperatures 30–50 K.

We identify the low-temperature set of lines as caused by electron transitions from a shallow donor to the YL-related defect. These lines will be called the DAP lines, although there is a possibility that the YL band is caused by transitions between shallow donors and deep donors at low temperature. In the latter case, the shift of the lines with excitation intensity can be explained by a gradual saturation of pairs with the shallow donor levels located farther from the conduction band (which have more localized wave functions and longer recombination times) if the shallow donors form a band with a width of about 10–20 meV due to their interaction. Another set of lines (Fig. 5), blueshifted by about 20 meV, appears at $T > 25$ K and is caused by transitions from the conduction band to the same deep-level defect. These transitions will be called e-A transitions even if the deep-level defect is a donor.

Figure 6 shows the energy difference between the DAP and e-A peaks of the YL and UVL bands as a function of excitation intensity. The distance between peaks is about 17–19 meV at the lowest excitation intensity and it decreases by about 5 meV as the excitation intensity increases by four orders of magnitude. These values are consistent with the ionization energy of the shallow donors in GaN (about 30 meV), after accounting for the effective Coulomb interaction for DAP in GaN with a concentration of donors of about 10^{17} cm^{-3} [2,14].

The distance between e-A and DAP peaks for the UVL band is slightly larger than that for the YL band (Fig. 6), because the PL lifetime of the UVL band (7–22 μs at 100 K for the samples used in Fig. 6) is shorter than that of the YL band (200–630 μs), and the excitation intensity necessary to saturate a particular DAP increases with decreasing PL lifetime. Given the same spatial separation between a shallow donor and acceptor in a DAP, PL via a deep acceptor (as is the case for the YL band) is expected to saturate at lower excitation intensity than PL via a shallow acceptor (the UVL band), and the ratio of these critical excitation intensities is expected to be equal to the inverse ratio of the PL lifetimes [15]. This explains why, for the same excitation intensity, the energy difference between the DAP and e-A peaks for the UVL is greater than that for the YL peaks.

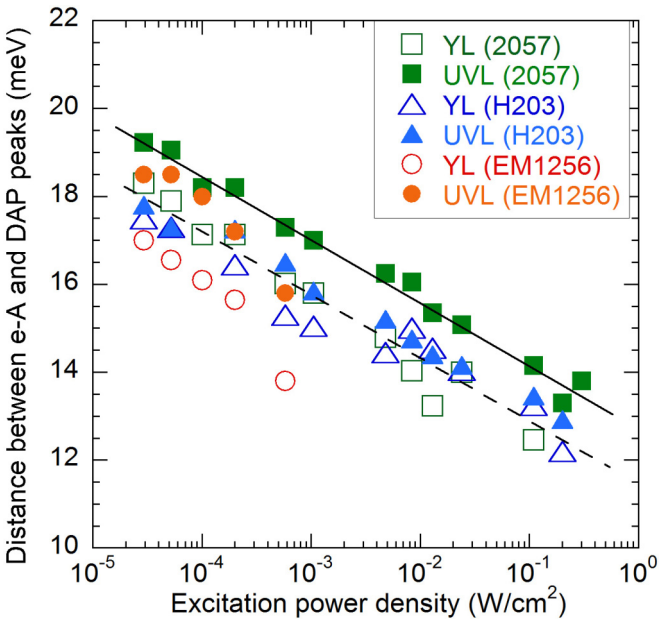

FIG. 6. Distance between DAP- and (e-A)-type ZPLs as a function of excitation intensity at 18 K for the UVL (filled symbols) and YL (empty symbols) bands in selected GaN samples. Positions of the e-A peaks were determined at temperatures between 30 and 50 K and extrapolated to 18 K. The solid and dashed lines, drawn to guide the eye, show the distances between e-A and DAP peaks for the UVL and YL bands, respectively, in sample H2057.

The thermodynamic transition level of the defect responsible for the YL band can be determined in the following way (the numbers are given for sample H2057 as an example). The ZPL at 2.571 eV (at 18 K) for the YL band corresponds to DAP transitions involving a shallow donor and a deep-level defect. The ZPL at 2.593 eV (at 40 K) corresponds to e-A transitions involving the same defect. Assuming that the e-A peak shifts with temperature as $0.5kT$ (which agrees with the observed shift of the e-A peak between 30 and 60 K), the (e-A)-related ZPL at 0–10 K is expected to be located at 2.590 eV. Since the DBE peak in this sample (3.473 eV) is shifted by 2 meV from its position in unstrained, bulk GaN (3.471 eV), and the band gap in the latter is 3.504 ± 0.001 eV (in agreement with the DBE and FE binding energies of 7 and 26 ± 1 meV, respectively) [2,16–18], the band gap in sample H2057 is $E_g = 3.506$ eV. Then, the thermodynamic transition level of the defect responsible for the YL band can be found as $E_A = E_g - E_0 = 0.916$ eV in the low-temperature limit.

We were able to find less-resolved ZPL and phonon-related fine structure of the YL band in several undoped GaN samples grown by HVPE (Table II). The band gap in these samples varied from 3.503 eV (thick, unstrained GaN) to 3.509 eV. The ZPLs in these samples are caused by DAP transitions at low temperature and are observed at photon energies between 2.564 eV and 2.574 eV at low excitation intensity. After finding the (e-A)-related ZPLs, we have estimated the position of the transition energy level of the YL-related defect. This value is $E_A = 0.916 \pm 0.003$ eV and is almost insensitive to the band gap variation. For the shallow acceptor responsible for the UVL band, $E_A = 0.223 \pm 0.003$ eV. The main source of the errors in these estimates is the extrapolation of the e-A line position from the temperature range of 25–40 K to the temperature range of 0–20 K.

We also resolved the ZPL and phonon-related fine structure for GaN samples grown by MOCVD, both undoped and Si doped. For undoped GaN (EM1256), the small GaN layer thickness resulted in a relatively large band gap (3.513 eV) and slightly larger DAP-related ZPL values (due to stress in the thin GaN layer) than for thicker GaN layers grown by HVPE (Table II). However, the values of E_A (0.918 eV for the YL band and 0.224 eV for the UVL band) are virtually the same as for HVPE GaN. The discovery that the YL band in MOCVD-grown GaN is identical to the YL band in HVPE-grown GaN (identical shape and fine structure) has important consequences, because in the latter it is difficult to resolve and study the behavior of the YL band, while in the former the YL band is well studied [4,5,19]. In particular, it has been established that the YL band in sample EM1256 is quenched at temperatures above 450 K with an activation energy of 0.85 eV. It also appears that the YL center is the same defect as the H1 trap identified by capacitance techniques [20].

TABLE II. Parameters of GaN samples and PL at $T = 18$ K and $P_{exc} = (1–5) \times 10^{-4}$ W/cm^2.

Sample number	Growth method	Thickness (μm)	Doping, N_D or N_A (cm^{-3})	E_g (eV)	YL E_0[a] (eV)	UVL E_0[a] (eV)	YL E_A (eV)
H2057	HVPE	24		3.506	2.571	3.262	0.916
H104	HVPE	10.6		3.505	2.570	3.261	0.916
H201	HVPE	15.3		3.508	2.574	3.265	0.916
H202	HVPE	20.4		3.509	2.574	3.266	0.917
H203	HVPE	21		3.509	2.574	3.266	0.917
H1007	HVPE	22		3.509	2.573	3.263	0.917
H3	HVPE	7		3.509	2.575	3.264	0.916
B73	HVPE	200		3.503	2.564	3.257	0.915
EM1256	MOCVD	1.9	C $\approx 4 \times 10^{16}$	3.513	2.577	3.268	0.918
cvd3540	MOCVD	5.5	Si $\approx 6 \times 10^{17}$	3.518	2.590	3.284	~0.928
cvd3784	MOCVD	12.5	Si $\approx 3 \times 10^{18}$	3.512	2.594	3.288	~0.918
cvd3533	MOCVD	5.8	Si $\approx 7 \times 10^{18}$	3.519	2.596	3.290	~0.923

[a]Positions of the ZPLs, which are DAP lines except for Si-doped samples, for which the emission peaks are identified as e-A transitions or an unresolved mixture of DAP and e-A transitions.

The ZPLs of the YL and UVL bands in Si-doped GaN (cvd3784) are located at 2.594 eV and 3.286 eV, respectively, at 18 K. They are broader, and the phonon-related fine structure is less well resolved but very similar to that in undoped GaN (Fig. 5). In contrast to the undoped GaN samples, no other peaks emerge at the high-energy side of the YL and UVL ZPLs with increasing temperature. We attribute the observed lines to (e-A)-type transitions in the Si-doped, degenerate GaN sample where shallow donor levels merge with the conduction band. This attribution is supported by the fact that the decay of both the YL and UVL after pulsed excitation is nearly exponential at 18 K in Si-doped GaN. In contrast, for undoped GaN, the decay of the UVL and YL is nonexponential at 18 K and becomes nearly exponential only at temperatures above 50 K when e-A transitions dominate over DAP transitions.

The values of E_A for the YL and UVL bands in Si-doped GaN sample cvd3784 (918 and 224 meV, respectively) are very close to the values obtained for undoped GaN. For GaN with a lower concentration of Si (sample cvd3540) the values of E_A for the YL and UVL bands (928 and 234 meV, respectively) are well outside the range of error. This may indicate that the defect-related PL lines in this sample are caused by unresolved superposition of DAP and e-A transitions.

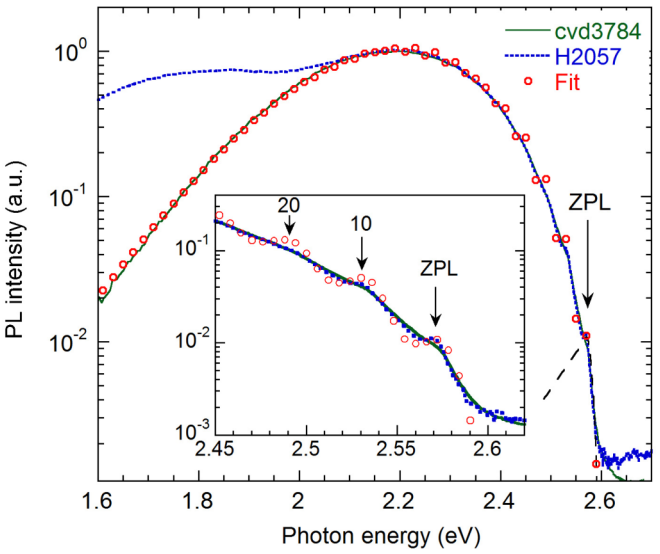

FIG. 7. Normalized SSPL spectra at $T = 18$ K and $P_{exc} = 1$ mW/cm^2 from Si-doped GaN (the solid line, sample cvd3784) and undoped GaN grown by HVPE (the dotted line, sample H2057). The spectrum of the sample cvd3784 is redshifted by 23 meV. The GL band is subtracted. The empty circles show the dependence calculated using Eq. (2) with parameters $S_1 = 4$ and $S_2 = 2$. The inset shows a zoomed-in region near the ZPL.

IV. DISCUSSION

A. Shape of the YL band

In Sec. III, we simulated the shape of the YL band using a one-dimensional configuration coordinate model which assumes that the large number of vibrational modes contributing to the PL band shape can be replaced by a single *effective* mode with energy $\hbar\Omega$. Previously, the value of $\hbar\Omega = 52$ meV was reported for the YL defect in the excited state [21]. In the current work, the dependence of the YL band FWHM on temperature between 15 and 650 K for several MOCVD samples reveals the value of $\hbar\Omega = 56 \pm 2$ meV. The shape of the YL band can be simulated using Eq. (1) with $S_e = 7.4$, $E_0 = 2.63$ eV, and $\hbar\omega_{max} = 2.20$ eV (Figs. 2–4). The above parameters are useful because they serve as fingerprints of the YL band. However, their physical meaning is limited, because two phonon modes contribute to the YL band shape, as can be seen in the fine structure.

Alternatively, for the case of multiple phonon modes, we can simulate the shape and find the Huang-Rhys factors corresponding to each phonon mode by using the approach described in [22]. The ZPL is expected to be very narrow at low temperature; however, it is broadened by inhomogeneities in the crystal structure and by interaction with lattice vibrations such as acoustic phonons. In the case of two vibrational modes, the intensities of the ZPL and its phonon replicas corresponding to the emission of m pseudolocal and n lattice phonons, W_{mn}, are given by

$$W_{mn} \propto \frac{S_1^m}{m!}\frac{S_2^n}{n!}, \tag{2}$$

where S_1 and S_2 are the Huang-Rhys factors describing the coupling with the two vibrational modes. Equation (2) is obtained assuming that the excited and ground vibrational states are identical parabolas with the same phonon frequencies [22]. If we neglect anharmonic interactions between vibrations, the shapes of all replicas are expected to be identical to the shape of the ZPL. The phonon replicas corresponding to the emission of $m + n$ phonons create peaks in the PL spectrum which are shifted to lower energies from the ZPL by distances $m\hbar\Omega_1 + n\hbar\Omega_2$, where $\hbar\Omega_1$ and $\hbar\Omega_2$ are the energies of the pseudolocal and lattice LO phonons, respectively.

The YL band shape simulated using Eq. (2) with $S_1 = 4$ ($\hbar\Omega_1 = 39.5$ meV) and $S_2 = 2$ ($\hbar\Omega_2 = 91.5$ meV) is shown in Fig. 7 by empty circles. The shape of the phonon replicas is identical to that of the ZPL which was arbitrarily simulated (the dashed curve in Fig. 7). The overall band shape obtained using Eq. (2) is very similar to the band shape obtained with Eq. (1) (Figs. 2–4). To reiterate, Eq. (1) is derived using a semiclassical approximation in which a vertical transition in a configuration coordinate diagram ends at the potential curve of the ground state, as in the case of a classical oscillator. This does not account for discrete energy levels of the vibrational system. On the other hand, Eq. (2) accounts for two vibrational modes, but it assumes that Huang-Rhys factors and phonon energies in the excited and ground states are the same and that the phonon replicas have exactly the same shape as the ZPL, which is arbitrarily simulated in our analysis.

The values of $S_1 = 4$, $\hbar\Omega_1 = 39.5$ meV, and $S_2 = 2$ for the YL band can be compared to the values of $S_1 = 1.5$, $\hbar\Omega_1 = 36$ meV, and $S_2 = 2$ for the BL band in GaN (related to the Zn_{Ga} acceptor) [2,23]. The intensity of the ZPL relative to the intensity of the band maximum is about 1% for the YL band and about 25% for the BL band. The small relative intensity of the ZPL for the YL band makes it difficult to observe, as opposed to the BL band in undoped GaN, which often clearly shows the ZPL and phonon-related fine structure.

The discovery of the ZPL and phonon-related fine structure for the YL band enables its reliable identification in different

samples. Previously, the ZPL was overlooked because its intensity is very low, and it is often buried under PL background produced by other emission bands. The observation of the ZPL also requires a low concentration of defects in GaN, which can be achieved in thick GaN layers grown by HVPE (such as the one with the PL spectrum shown in Fig. 2).

B. The origin of the YL band

From our experiments, the exact origin of the YL band cannot be established. Nevertheless, very important information about the related defect is obtained which will serve as a rigid constraint for future explanations. The most important findings are the following:

(1) Several defects may produce broad PL bands with a maximum in the range of 2.1–2.3 eV. The band identified in this work will be called the YL1 band (or the YL1 center/defect), hereafter.

(2) The YL1 band has the following parameters and properties. Its slightly asymmetric shape at low temperatures can be simulated using Eq. (1) with $S_e = 7.4$, $E_0^* = 2.66$ eV, and $\hbar\omega_{\max} = 2.20$ eV. At low temperature, the YL1 ZPL at 2.57 eV is followed by two sets of phonon replicas: a pseudolocal mode with $S_1 = 4$ and $\hbar\Omega_1 = 39.5$ meV and the LO lattice vibrational mode with $S_2 = 2$ and $\hbar\Omega_2 = 91.5$ meV. The intensity of the ZPL is 0.01 of the intensity of the YL1 band maximum. The ZPL at 18 K is caused by DAP-type electron transitions from a shallow donor to a deep defect whose thermodynamic transition level is located at 0.916 ± 0.003 eV above the valence band maximum. At elevated temperatures ($T > 40$ K) the DAP-related lines are replaced with (e-A)-related lines; i.e., transitions from the conduction band to the same defect level begin to dominate.

(3) The YL1 center is responsible for the dominant YL band in undoped GaN grown by MOCVD, Si-doped GaN grown by MOCVD, and undoped GaN grown by HVPE. It is very likely that the defect is an acceptor, because the DAP-type behavior of the YL1 band is identical to that of the UVL band, which is caused by a shallow acceptor.

(4) The YL1 band and the GL band are related to different defects. This conclusion follows from the fact that the saturation of the YL1 band at high excitation intensity does not result in the appearance of the GL band in MOCVD-grown GaN samples, whereas the GL band is observed in HVPE-grown GaN and does not exhibit any correlation with the YL1 band intensity.

The experimentally found parameters of the YL1 band [the band maximum $\hbar\omega_{\max}$, the thermodynamic transition level E_A relative to the valence band maximum, and the ZPL position E_0 for (e-A)-type transitions] can be compared with recent theoretical predictions made by several research groups (Table III) [3–6,24]. Below, we will review arguments in favor of or against the attribution of the YL1 band to a particular defect and will raise questions for theorists.

1. *Isolated* C_N

Lyons *et al.* [3], by employing hybrid functionals within density functional theory and using a 96-atom supercell, have calculated that C_N is a deep acceptor in GaN with the $-/0$ transition level at 0.90 eV above the valence band maximum,

TABLE III. Comparison of parameters of the YL1 center with parameters of several defects predicted from first-principles calculations.

Defect	$\hbar\omega_{\max}$ (eV)	E_0 (eV)	E_A (eV)	Source
YL1 center	2.22	2.59	0.916	This work
C_N	2.14	2.60	0.90	[3]
C_N	1.98	2.45	1.04	[5]
C_N	2.18	2.67	0.78	[24]
C_NO_N	2.25	2.73	0.75	[4,5]
C_NO_N	2.28	2.77	0.68	[24]
C_NSi_{Ga}	2.44	2.94	0.51	[24]
V_{Ga}	2.27	2.80	2.80	[6]
V_{Ga}-3H	2.05	2.77	0.73	[6]
$V_{Ga}O_N$-2H	1.90	2.58	0.92	[6]

which gives rise to a YL band with a maximum at 2.14 eV and the ZPL at 2.60 eV. Later, Christenson *et al.* [24] refined these parameters for C_N (Table III) by including the semicore Ga $3d$ electrons as valence electrons and using a larger 300-atom supercell. The parameters roughly agree with the parameters of the YL1 center. However, the C_N center is also expected to have a $0/+$ transition level at 0.35 eV [25] or at 0.48 eV [5] above the valence band maximum. In this case, by increasing the excitation intensity, one would observe the saturation of the YL band (the "primary band" caused by transitions via the $-/0$ level) and the rise of another emission band at higher photon energies (a "secondary band" caused by transitions via the $0/+$ level). First-principles calculations predict that this secondary band is blue or green, with $\hbar\omega_{\max} = 2.70$ eV and $E_0 = 3.15$ eV [25] or $\hbar\omega_{\max} = 2.59$ eV and $E_0 = 3.0$ eV [5]. However, in our MOCVD-grown samples, both undoped and Si doped, no secondary band emerges after saturation of the YL1 band occurs (see, for example, Fig. 2 in Ref. [5]). An explanation can be suggested that the quantum efficiency of the secondary band is too low to be detected in the PL spectrum due to a very low hole-capture cross section by the C_N defect in its neutral state. Since the peak intensity of the YL1 band is at least 10^3 times higher than the background PL intensity in the photon energy region where the secondary band is expected, the explanation requires that $C_{pA} < 6 \times 10^{-10}$ cm^3/s for the hole capture by C_N^0. An alternative explanation is that the recombination of electrons with holes at the C_N^+ defects is nonradiative. We cannot exclude also the possibility that that the $0/+$ level of C_N is much closer to the valence band than predicted or does not exist at all.

If the YL1 band is caused by the isolated C_N defect, then the question arises: "Which defect is responsible for the strong GL band in HVPE-grown GaN?" Previously, we identified the GL band ($\hbar\omega_{\max} = 2.40$ eV and $E_0 \approx 2.9$ eV) as the secondary band of the C_N defect because its intensity increased as the square of the excitation intensity, as one would expect for a defect capturing two holes before radiative recombination takes place [5]. This attribution agrees with calculated transition energy levels for C_N [5], as well as with the giant-trap-like behavior of the Coulombic excited level of the positively charged state of the defect responsible for the GL [26]. In the current work we find that the YL1 band cannot be the primary band for a defect giving rise to the GL band. It

is possible that another YL band (unresolved in the PL spectra from HVPE-grown GaN) or a red PL band is the primary emission band for the GL. We cannot also exclude the possibility that the primary transition is nonradiative.

2. C_NO_N and C_NSi_{Ga} complexes

We suggested previously that the isolated C_N defect is responsible for the YL and GL bands in HVPE-grown GaN, whereas the C_NO_N complex is responsible for the YL band in MOCVD-grown GaN [4,5]. In addition to first-principles calculations favoring such identifications, we argued that the isolated C_N defect should cause two PL bands due to two charge transition levels of C_N in GaN, while the C_NO_N complex is expected to produce only one PL band [5]. The results of the current work question the attribution of the YL1 band to the C_NO_N complex. First, the shift of the YL1 band with excitation intensity (Fig. 6) is easier to explain by the DAP-type transition, where an electron from a shallow donor recombines with a hole bound to a deep acceptor. For the C_NO_N complex, it is necessary to assume that the shift of the PL band is caused by transitions from shallow donors, with a distribution of energy levels, to the deep C_NO_N donor, in which case the shift is not necessarily similar to the one for a DAP band.

Another experimental fact to be explained is that the YL1 center is the dominant radiative defect in both undoped GaN (sample EM1256) and Si-doped GaN samples. Both C_NO_N and C_NSi_{Ga} are expected to give rise to broad PL bands that would be easy to distinguish in an experiment, because the C_NSi_{Ga} complex is expected to have a maximum (and the ZPL) at higher photon energies, by about 0.17 eV [24]. Christenson *et al.* [24] predict that in undoped GaN the concentration of both complexes is much lower than the concentration of isolated C_N because of the small binding energy in these complexes. They also argue that the binding energy in the C_NO_N complex is smaller than that in the C_NSi_{Ga} complex, which would result in a higher concentration of the C_NSi_{Ga} complexes, especially in Si-doped GaN. Since the same YL1 band dominates in both undoped and Si-doped GaN, it seems unlikely to be caused by the C_NO_N complex and, between the two choices, should rather be attributed to the C_NSi_{Ga} complex according to the predictions of Ref. [24]. However, the calculated ZPL for the C_NSi_{Ga} complex (2.94–2.96 eV [24]) disagrees with the experimental value for the YL1 band (2.59 eV).

3. V_{Ga} and V_{Ga} complexes

Lyons *et al.* [6] suggested that one of the YL bands may be caused by the isolated gallium vacancy (V_{Ga}), namely, by the radiative capture of holes from the valence band to an acceptor level located at 0.70 eV below the conduction band. In principle, such a mechanism is possible, although the *observation* of the related PL band in *n*-type GaN is highly unlikely. Indeed, photogenerated holes are either captured very quickly by radiative and nonradiative defects or form excitons in *n*-type GaN (faster than 1 ns), whereas the optical transitions causing experimentally observed YL bands are typically very slow (slower than 100 μs for undoped GaN). In this case, the intensity of the PL band would be extremely weak and it would not be observed in PL spectra. On the other hand, the V_{Ga}-containing complexes, V_{Ga}-3H and $V_{Ga}O_N$-2H, appear to be reasonable candidates for the YL band [6]. However, since both complexes are deep donors, the DAP-type shift of the YL1 band with excitation intensity (Fig. 6) should be addressed, in the same manner as for other deep donors such as C_NO_N and C_NSi_{Ga}.

The YL1 center may not be the only defect that gives rise to PL bands in the emission spectrum near 2.2 eV. Unfortunately, detailed information about other YL bands (including the ZPL and the strength of electron-phonon coupling) is apparently not available in the literature. The YL band in high-resistivity GaN doped with C [27] has a maximum at about 2.24 eV and a shape very similar to the YL1 band shape. Note that the shape and position of this band were used in Ref. [6] for comparison with theoretical calculations. In our high-resistivity GaN samples doped with C, the YL band maximum is also observed at 2.24 eV, yet the exciton peaks (and therefore the band gap) in these MOCVD-grown GaN layers are blueshifted by about 25 meV. The fine structure of the YL band cannot be observed in these samples because of the strong BL2 band, so that the identity of the YL band in C-doped, high-resistivity GaN as being the YL1 center can be neither confirmed nor rejected.

Finally, we would like to note that the relatively high quantum efficiency of the YL1 band for sample H2057 (Fig. 1) and low concentration of carbon impurity in this sample (at least an order of magnitude lower than in MOCVD-grown samples; see Table I) do not contradict the attribution of the YL1 band to a carbon-related defect. Indeed, PL intensity is proportional to the concentration of associated defects only for low concentrations of the defects, often below the detection limit of SIMS measurements for impurities. For example, the absolute quantum efficiency of the Zn-related blue luminescence in undoped and Zn-doped GaN increases linearly with the concentration of Zn atoms and reaches 30% for [Zn] $\approx 10^{16}\,\mathrm{cm}^{-3}$ [20]. At higher concentrations of Zn atoms, the quantum efficiency approaches 100% for some samples or stays at 30% for others, apparently due to the uncontrolled incorporation of nonradiative defects.

V. CONCLUSION

We described in detail the properties of the yellow luminescence band in GaN labeled as YL1. The ZPL of the YL1 band is found at 2.590 ± 0.003 eV with an intensity of about 1% from the YL1 band maximum (located at 2.22 eV for electron transitions from the conduction band). The fine structure at the high-energy side of the YL1 band includes a set of peaks formed by the superposition of two phonon modes: a pseudolocal mode with phonon energy of 39.5 meV and a lattice LO phonon mode (91.5 meV). We conclude that, in undoped GaN grown by HVPE, in undoped GaN grown by MOCVD with carbon as the dominant acceptor, and in Si-doped GaN grown by MOCVD with concentrations of Si up to $7 \times 10^{18}\,\mathrm{cm}^{-3}$, the yellow band is caused by the same defect—the YL1 center.

ACKNOWLEDGMENTS

The authors thank Denis Demchenko for fruitful discussions. The work was supported by the National Science Foundation (Grant No. DMR-1410125).

[1] C. Freysoldt, B. Grabowski, T. Hickel, J. Neugebauer, G. Kresse, A. Janotti, and C. G. Van de Walle, Rev. Mod. Phys. **86**, 253 (2014).
[2] M. A. Reshchikov and H. Morkoç, J. Appl. Phys. **97**, 061301 (2005).
[3] J. L. Lyons, A. Janotti, and C. G. Van de Walle, Appl. Phys. Lett. **97**, 152108 (2010).
[4] D. O. Demchenko, I. C. Diallo, and M. A. Reshchikov, Phys. Rev. Lett. **110**, 087404 (2013).
[5] M. A. Reshchikov, D. O. Demchenko, A. Usikov, H. Helava, and Yu. Makarov, Phys. Rev. B **90**, 235203 (2014).
[6] J. L. Lyons, A. Alkauskas, A. Janotti, and C. G. Van de Walle, Phys. Status Solidi B **252**, 900 (2015).
[7] T. Ogino and M. Aoki, Jpn. J. Appl. Phys. **19**, 2395 (1980).
[8] M. A. Reshchikov, R. J. Molnar, and H. Morkoç, in *Wide Bandgap Electronics*, MRS Symposium Proceedings No. 680, edited by T. E. Kazior, P. P. Parikh, C. Nguyen, and E. T. Yu (Materials Research Society, Warrendale, PA, 2001), p. E5.6.
[9] M. A. Reshchikov, A. A. Kvasov, M. F. Bishop, T. McMullen, A. Usikov, V. Soukhoveev, and V. A. Dmitriev, Phys. Rev. B **84**, 075212 (2011).
[10] M. A. Reshchikov, M. A. Foussekis, J. D. McNamara, A. Behrends, A. Bakin, and A. Waag, J. Appl. Phys. **111**, 073106 (2012).
[11] M. A. Reshchikov, D. O. Demchenko, J. D. McNamara, S. Fernández-Garrido, and R. Calarco, Phys. Rev. B **90**, 035207 (2014).
[12] A. Alkauskas, J. L. Lyons, D. Steiauf, and C. G. Van de Walle, Phys. Rev. Lett. **109**, 267401 (2012).
[13] E. Zacks and A. Halperin, Phys. Rev. B **6**, 3072 (1972).
[14] A. Wolos, Z. Wilamowski, M. Piersa, W. Strupinski, B. Lucznik, I. Grzegory, and S. Porowski, Phys. Rev. B **83**, 165206 (2011).
[15] M. A. Reshchikov, J. Appl. Phys. **115**, 103503 (2014).
[16] B. Monemar, Phys. Rev. B **10**, 676 (1974).
[17] K. Reimann, M. Steube, D. Fröhlich, and S. J. Clarke, J. Cryst. Growth **189-190**, 652 (1998).
[18] B. Monemar, P. P. Paskov, J. P. Bergman, A. A. Toropov, and T. V. Shubina, Phys. Status Solidi B **244**, 1759 (2007).
[19] M. A. Reshchikov, Appl. Phys. Lett. **88**, 202104 (2006).
[20] M. A. Reshchikov, in *Point defects in GaN*, in *Semiconductors and Semimetals: Defects in Semiconductors*, edited by C. Jagadish, V. Privitera, and L. Romano (Academic Press, Burlington, UK, 2015), Vol. 91, pp. 315–367.
[21] M. A. Reshchikov, F. Shahedipour, R. Y. Korotkov, M. P. Ulmer, and B. W. Wessels, Physica B **273-274**, 105 (1999).
[22] K. K. Rebane, *Impurity Spectra of Solids* (Plenum, New York, 1970), p. 68.
[23] M. A. Reshchikov, F. Shahedipour, R. Y. Korotkov, M. P. Ulmer, and B. W. Wessels, J. Appl. Phys. **87**, 3351 (2000).
[24] S. G. Christenson, W. Xie, Y. Y. Sun, and S. B. Zhang, J. Appl. Phys. **118**, 135708 (2015).
[25] J. L. Lyons, A. Janotti, and C. G. Van de Walle, Phys. Rev. B **89**, 035204 (2014).
[26] M. A. Reshchikov, J. D. McNamara, A. Usikov, H. Helava, and Yu. Makarov, Phys. Rev. B **93**, 081202(R) (2016).
[27] C. H. Seager, D. R. Tallant, J. Yu, and W. Götz, J. Lumin. **106**, 115 (2004).